Information Theoretical Limits for Quantum Optimal Control Solutions: Error Scaling of Noisy Channels

Matthias M. Müller, Stefano Gherardini, Tommaso Calarco, Simone Montangero, Filippo Caruso

***Abstract*—Accurate manipulations of an open quantum system require a deep knowledge of its controllability properties and the information content of the implemented control fields. By using tools of information and quantum optimal control theory, we provide analytical bounds (information-time bounds) to characterize our capability to control the system when subject to *arbitrary* sources of noise. Moreover, since the presence of an external noise field induces an open quantum system dynamics, we also show that the results provided by the information-time bounds are in perfect agreement with the Kofman-Kurizki universal formula describing decoherence processes. Finally, we numerically test the universal scaling of the control accuracy as a function of the noise parameters, by using the dressed chopped random basis (dCRAB) algorithm for quantum optimal control.**

***Index Terms*—Open quantum systems, Quantum optimal control, Channel capacities, Quantum speed limit, decoherence.**

I. INTRODUCTION

A quantum system is defined as open when it interacts with other systems or an environment with several degrees of freedom. Such an interaction radically changes the dynamics of the system, e.g., making the dynamics propagator a non-unitary operator [1], [2]. The semi-classical effects of the interaction between a quantum system and the external environment can be reliably modeled by adding stochastic noise fields acting on operators governing the Hamiltonian evolution of the quantum system. As a result, the evolution of the system turns out to be described by stochastic quantum dynamics, e.g., the stochastic Schrödinger equation, generating as solutions the functionals that are usually known as quantum trajectories [3], [4], [5], [6], [7], [8]. An example of a relevant noise source, especially in biological and solid-state systems, is provided by the $1/f$ noise [9], [10]. This kind of noise, which decreases as a function of the frequency with a hyperbolic trend, is usually responsible for destroying the phase coherence terms of quantum operations implemented in solid-state devices [11]. In order to prevent it, the prediction of the spectral properties on the external noise sources [12], [13], [14], [15], e.g., by means of quantum estimation methods [16], is going to play a key role to enhance the performance of quantum technology devices [17].

M.M. Müller is with Forschungszentrum Jülich GmbH, Peter Grünberg Institute - Quantum Control (PGI-8), D-52425 Jülich Germany.

S. Gherardini and F. Caruso are with the Department of Physics & Astronomy & LENS, University of Florence, I-50019 Sesto Fiorentino, Italy.

T. Calarco is with Forschungszentrum Jülich GmbH, Peter Grünberg Institute - Quantum Control (PGI-8), D-52425 Jülich Germany and with the Institute for Theoretical Physics, University of Cologne, D-50937 Cologne, Germany.

S. Montangero is with the Department of Physics & Astronomy "G. Galilei", University of Padua, and with INFN Sezione di Padova, I-35131 Padua, Italy.

To tackle efficiently the problem of steering a noisy quantum system in a desired way, a variety of solutions have been introduced. A widely used tool to mitigate the detrimental effect of the interaction of a system with its environment is provided by dynamical decoupling (DD) of the system from the environment [18]. This approach allows to enhance or suppress certain desired interaction modes [19], [20], [21], [22], [23], [24] and the protocols can also be optimized by analytic or numeric optimization algorithms [25], [26], [27], [28]. A different approach which we will also follow in this article, is the extension of quantum optimal control (QOC) methods [29], [30], [31], [32] to open quantum systems [33], [34], [35], [36], [37], [38], [39], [40], [41]. Commonly used algorithms for QOC include Krotov [42] gradient ascent pulse engineering (GRAPE) [43] and optimization in the chopped random basis (CRAB) [44], [45], e.g., following the dressed CRAB (dCRAB) algorithm [46].

The smoothness and bandwidth of the QOC solution is an important constraint that can be included in the QOC algorithm. The CRAB/dCRAB algorithm naturally produces a bandwidth-limited solution by making an ansatz for the solution using a basis with the desired properties. Such a spectrally-limited control has been achieved also with gradient-based QOC algorithms such as Krotov [47] and GRAPE [48] through filters in the update formula. Alternatively, also the CRAB-ansatz can be combined with gradient optimization. The gradient-based algorithms of the CRAB family are known as gradient optimization using parametrization (GROUP) and a comparison is undertaken in Ref. [49]. In this article we employ the dCRAB algorithm [44], [45], [46], which has been successfully demonstrated experimentally on different quantum platforms [41], [50], [51], including the use of closed-loop optimization [52], [53], [54].

An important limit for any quantum control solution is given by a time-energy bound known as quantum speed limit (QSL) [55], [56] that fundamentally reflects the time-energy uncertainty relation. It can be formulated also for open quantum systems [57] and its effect can be observed by QOC when the pulse operation time approaches the theoretical QSL [58].

Another bound is given by the information content of the control pulse: in Ref. [59] a so-called "$2M-2$-rule" (M being the dimension of the quantum system) for the degrees of freedom of the control field could be confirmed by studying numerically different QOC problems. Later this could be found also for quantum many-body systems [60]. Arguments based on information theory allowed to quantify the information content of a control field and to introduce bounds on the control error and minimum pulse operation time [61]. Indeed, by using the tools from classical and quantum information theory [2], [62], [63], [64], one can consider the control pulse as a communication signal whose correct reception means the achievement of the desired control task with suitably small error. The same reasoning applies also when the control over the quantum system is achieved through another quantum system, considering the quantum communication channel from the controlling quantum system to the controlled quantum system [65].

It is worth noting that any communication channel is subjected to (usually correlated) external noise sources that have the effect of degrading the transmitted signals or losing information packets. However, the modeling of such signal degradation has allowed to understand the processes underlying system-noise field interactions, as for example in [66] where correlated quantum dynamics, also leading to non-Markovian evolutions, has been analyzed with an information theory perspective.

In this paper, we assume that one or more noise sources affect the internal Hamiltonian of the quantum system under analysis, governing the coherent part of its dynamical evolution. This means that the interaction between the system and the external environment leads to extra non-deterministic terms proportional to an external stochastic field, modeled by a stochastic Schrödinger equation as previously described. Thus, after deriving the master equation governing the mean stochastic dynamics of the system, averaged over the noise realization, we evaluate the channel capacity associated to an optimal control problem, whereby the optimized control pulse acts on the noisy quantum system. According to Shannon's theorems [63], [64], the values of the corresponding channel capacity in the frequency domain strictly depend on the noise power spectral density, as well as the control error in reaching a desired quantum state. In particular, in this paper the relations between these quantities are quantitatively characterized, both analytically and by means of numerical simulations, and we show that they are in agreement with the Kofman-Kurizki universal formula for decoherence in quantum processes [19], [20].

II. Control Problem

A. System Dynamics

We consider a quantum system described by a state $\rho(t)$, where the time evolution is given by a stochastic Schrödinger equation (SSE)

$$\dot{\rho} = -i[H(t), \rho]\,. \tag{1}$$

Here, the Hamiltonian

$$H(t) = H_d + f(t)H_c + \xi(t)H_n \tag{2}$$

consists of a drift term H_d, a control term $f(t)H_c$ (with control operator H_c and control field $f(t)$) and a stochastic noise term $\xi(t)H_n$ (where H_n is a fixed operator and $\xi(t)$ is a stochastic field).

B. Control Objective

The goal of the quantum optimal control problem is to find the optimal control pulse $\hat{f}(t)$ driving the quantum system from the initial state $\rho(0)$ to the target state $\hat{\rho}$ at final time T. The optimization problem that provides $\hat{f}(t)$ does not necessarily have an exact solution. This necessarily entails a non-zero control error ε, meaning that the optimal control pulse does not perfectly drive the system to the target state $\hat{\rho}$ but to a final state $\rho(T)$ in the ε-ball around the target state. The control error ε is commonly expressed as a function of the Uhlmann fidelity [67] $\mathfrak{F}(\hat{\rho}, \langle\rho(T)\rangle)$ between the target state and the final state, i.e., $\varepsilon \equiv 1 - \mathfrak{F}(\hat{\rho}, \langle\rho(T)\rangle)$, with

$$\mathfrak{F}(\hat{\rho}, \langle\rho(T)\rangle) \equiv \mathrm{Tr}\sqrt{\sqrt{\hat{\rho}}\langle\rho(T)\rangle\sqrt{\hat{\rho}}}. \tag{3}$$

Note that the averaging $\langle\cdot\rangle$ of the final state refers to the statistics of the noise field $\xi(t)$. From here on we omit this averaging unless explicitly stated.

C. Optimization Algorithm

In the example section we will study how well for specific control problems the control objective can be achieved by means of QOC. In particular, we will employ the dCRAB algorithm [46] to solve the optimization problem. This algorithm makes an ansatz for the optimal solution of the form

$$f(t) = \sum_{i=1}^{N_c} c_i f_i(t) \tag{4}$$

and the optimization is then performed on this subspace of smaller dimension. This can in principle be done by any direct search method: in this work we use the Nelder-Mead simplex algorithm [68] to find the optimal set of coefficients c_i ($i = 1, \ldots N_c$). To exploit the usually advantageous properties of the control landscape [31], [69] which could be distorted by the finite dimensional expansion, after convergence of the direct search method a basis change can be introduced and the optimization continued in an iterative way:

$$f^j(t) = c_0^j f^{j-1}(t) + \sum_{i=1}^{N_c} c_i^j f_i^j(t)\,, \tag{5}$$

where $f_i^j(t)$ are the new basis functions, and $f^{j-1}(t)$ is the optimal solution from the $(j-1)$th iteration. The coefficient c_0^j allows the optimization to move along the direction of the old pulse, while the coefficients c_i^j ($i = 1, \ldots, N_c$) allow it to move along the new search directions $f_i^j(t)$.

If we choose the basis functions $f_i^j(t)$ to be trigonometric functions with random frequencies ω_i^j and choose these frequencies to lie in an interval of a specified bandwidth, we can in a natural way incorporate a bandwidth constraint for $f(t)$. As we will see, we will also need to fix the pulse power, which can be done by simply rescaling the coefficients c_i^j (such that the desired pulse power is obtained) before calculating the system evolution.

III. Time-continuous Stochastic Schrödinger Equation and Master Equation

In this section we derive the Master equation obtained by averaging the SSE over the noise realizations. If we plug in the explicit form of the Hamiltonian, Eq. (2) into the Schrödinger equation (1), we obtain

$$\dot{\rho} = -i[H(t),\rho] = -i[H_d + f(t)H_c, \rho] - i[\xi(t)H_n, \rho]\,. \quad (6)$$

The integral form of the initial value problem is given by

$$\rho(t) = \rho(0) - i\int_0^t [H(t'),\rho(t')]dt', \quad (7)$$

which can be re-inserted into the differential equation leading to

$$\begin{aligned}\dot{\rho}(t) &= i[H_d + f(t)H_c, \rho] \\ &\quad -i\left[\xi(t)H_n, \left(\rho(0) - i\int_0^t [H(t'),\rho(t')]dt'\right)\right] \quad (8)\end{aligned}$$

The stochastic process $\xi(t)$ follows the distribution $p_t(\xi)$, whereby the mean value and the correlation function of $\xi(t)$ are respectively defined as $\langle\xi(t)\rangle = \int_\xi p_t(\xi)\xi d\xi$ and

$$R_\xi(t,t') \equiv \langle \xi(t)\xi'(t')\rangle = \int_\xi \int_{\xi'} p_{t,t'}(\xi,\xi')\xi\xi' d\xi d\xi'\,, \quad (9)$$

where $\langle\cdot\rangle$ denotes the averaging over the noise realizations. For $\langle\xi\rangle = 0$ we find, after averaging,

$$\begin{aligned}\dot{\rho}(t) &= -i\left[H_d + f(t)H_c, \rho(t)\right] \\ &\quad -\left[H_n, \left[H_n, \int_0^t R_\xi(t,t')\rho(t')dt'\right]\right]. \quad (10)\end{aligned}$$

Analogous results regarding stochastic dynamics in Hilbert spaces have been already found for instance in Ref. [1].

IV. Noise correlation function and power spectral density

A central role in the characterization of the SSE is given by our knowledge of the noise correlation function $R_\xi(t,t')$. In particular, in this paper we will investigate control problems involving quantum systems subjected to white noise as well as coloured ones, under the assumption of $\{\xi(t)\}_{t\in\mathbb{R}}$ being a weakly stationary stochastic process. This implies the following properties [71]:

(i) the mean value of ξ does not depend on the time instant t in which the noise field is sampled, i.e. $\int p_t(\xi)\xi d\xi = \int p_{t+t'}(\xi)\xi d\xi$, $\forall t' \in \mathbb{R}$.
(ii) the correlation function is translation invariant: $R_\xi(t,t') = R_\xi(t+t'', t'+t'')$ $\forall t'' \in \mathbb{R}$. This implies that we can write $R_\xi(t,t') = R_\xi(\tau)$, with $\tau = t - t'$.
(iii) the second moment of ξ is finite: $\int p_t(\xi)\xi^2 d\xi < \infty$ $\forall t' \in \mathbb{R}$.

As a result, the SSE reads

$$\begin{aligned}\dot{\rho}(t) &= -i\left[H_d + f(t)H_c, \rho(t)\right] \\ &\quad -\left[H_n, \left[H_n, \int_0^t R_\xi(t-t')\rho(t')dt'\right]\right]\,. \quad (11)\end{aligned}$$

It is worth noting that the case of non-stationary noise terms can be obtained by considering $\{\xi\}_{t\in\mathbb{R}}$ as a *piece-wise* stationary stochastic process.

A. Example: Master Equation for Gaussian White Noise

Let us assume that $\xi(t)$ is a Gaussian white noise field with zero mean value $\langle\xi(t)\rangle$ and correlation function

$$R_\xi(t-t') = 2\gamma\delta(t-t'). \quad (12)$$

Then, the SSE of Eq. (11) is described by the following master equation:

$$\dot{\rho}(t) = -i[H_d + f(t)H_c, \rho(t)] - 2\gamma\big[H_n, [H_n, \rho(t)]\big], \quad (13)$$

where the parameter γ stands for the noise strength. For instance, if we consider a two-level system and H_n is taken to be equal to the Pauli matrix $\sigma_z = \begin{pmatrix}1 & 0\\ 0 & -1\end{pmatrix}$, the SSE simply becomes

$$\dot{\rho}(t) = -i[H_d + f(t)H_c, \rho(t)] + \gamma\begin{pmatrix}0 & \rho_{12}(t)\\ \rho_{21}(t) & 0\end{pmatrix}\,. \quad (14)$$

Thus, this approach can be considered as the *microscopic* derivation of the pure-dephasing Gorini-Kossakowski-Sudarshan-Lindblad (GKSL) equation, as conventionally stated in the open quantum systems literature [1], [2].

V. Measures of signals information content

A. Signal-to-noise ratio

The signal-to-noise ratio is a measure used in statistical signal processing to compare the powers of a desired signal and an external noise source [72]. It is usually characterized in the frequency domain. By properly formalizing the signal-to-noise ratio, we are able to predict the amount of information carried by a specific signal embedded in a noisy environment. In our case the desired signal is represented by the control Hamiltonian $f(t)H_c$ (and in particular the deterministic time-dependent control field $f(t)$), while the noise is given by the noise Hamiltonian $\xi(t)H_n$, i.e. by the stochastic noise field $\xi(t)$.

The signal-to-noise ratio S/N is defined as the ratio of the power of the signal S and the power of the noise N. By introducing also the power P_f of the control field $f(t)$ and the power Σ_ξ of the stochastic noise field $\xi(t)$, we can define

$$S = P_f||H_c|| \;\text{ and }\; N = \Sigma_\xi||H_n||\,, \quad (15)$$

where, without loss of generality, we can set the operator norms to $||H_c|| = ||H_n|| = 1$ as the proportionality factors can be absorbed in $f(t)$ and $\xi(t)$. The signal-to-noise ratio can then be written as

$$\frac{S}{N} = \frac{P_f}{\Sigma_\xi}. \quad (16)$$

In Eq. (16), the power P_f of the control field is defined as

$$P_f \equiv \frac{1}{T}\int_0^T |f(t)|^2 dt\,, \quad (17)$$

where T is the duration of the control pulse. Using *Parseval's theorem* the power P_f of the control field can be expressed also in the frequency domain:

$$P_f = \frac{1}{2\pi}\int_{-\infty}^{\infty} \phi_f(\omega)d\omega, \quad (18)$$

where $\phi_f(\omega)$ denotes the power spectral density of $f(t)$, namely the Fourier transform of its auto-correlation function $R_f(\tau) \equiv \int_0^\infty f^*(t)f(t-\tau)dt$:

$$\phi_f(\omega) = \int_{-\infty}^{\infty} R_f(\tau)e^{-i\omega\tau}d\tau\,. \tag{19}$$

Likewise, we can define the power spectral density of the stochastic noise field as

$$\varphi_\xi(\omega) = \int_{-\infty}^{\infty} R_\xi(\tau)e^{-i\omega\tau}d\tau \tag{20}$$

and consequently the power Σ_ξ of the stochastic noise field as

$$\Sigma_\xi = \frac{1}{2\pi}\int_{\infty}^{-\infty} \varphi_\xi(\omega)d\omega\,. \tag{21}$$

In conclusion, the signal-to-noise ratio can be written as

$$\frac{S}{N} = \frac{\int_{-\infty}^{\infty}\phi_f(\omega)d\omega}{\int_{-\infty}^{\infty}\varphi_\xi(\omega)d\omega}\,. \tag{22}$$

B. Channel capacity

In Shannon information theory, a channel can asymptotically transmit a message without errors at the maximum rate $\mathcal{C}$, (channel capacity) [62]. Then, the information (in terms of number of bits) carried by the signal (in our case the control field $f(t)$) is defined as $I_f \equiv \mathcal{C}T$, with T the duration of the signal. The channel capacity thus quantifies the information carried by the maximum number $\mathcal{M}$ of distinguishable messages that can be reliably encoded and decoded in a communication procedure through this channel per unit time [62], [2].

In this paper, we specifically investigate how a control field can steer a quantum system, such that the state of the quantum system is transformed in a desired way. In such a QOC problem, the role of the decoded messages is played by the number of distinguishable states that can be reached and the encoded messages is replaced by the set of all admissible control fields $f(t)$. The communication channel then depends on the control landscape related to the specific quantum system dynamics [31], [69] and on the stochastic noise field. The information transferred to the system is given by the information encoded in the control field $f(t)$ reduced by the detrimental action of the stochastic noise field $\xi(t)$, while the specific control landscape reflects the ability of the quantum system to receive this information.

In this section, we investigate from an information theoretical perspective the channel capacity related to the transfer of information from the control apparatus onto the system, while for now we neglect the possibly limited ability of the system to utilize this information. This will give us an upper bound for the channel capacity of the global channel (i.e. from the control apparatus to the final state of the system dynamics). This intermediate step allows us to apply directly the seminal works of Shannon [63], [64] and has the advantage of not being affected by the limitations regarding the dimensionality and controllability of the quantum system.

1) Noiseless case: The channel capacity of the noiseless channel is given by *Hartley's law* [70]. In this case, what prevents $\mathcal{M}$ (the maximum number of distinguishable messages) from being infinite are (i) a finite dynamic range Δf of the amplitude of the encoded signal and (ii) inaccuracies in the signal. The former is related to the magnitude of the control, and the latter to the precision δf of the signal (i.e. as generated by the control electronics). Thus, Hartley's law states that in the noiseless case the channel capacity equals

$$\mathcal{C} = \Delta\Omega\log_2(\mathcal{M}) = \Delta\Omega\log_2\left(1+\frac{\Delta f}{\delta f}\right), \tag{23}$$

where $\Delta f/\delta f$ is generally denoted as the resolution of the pulse $f(t)$, while $\Delta\Omega = \omega_{\max} - \omega_{\min}$ is the channel bandwidth given by the minimal and maximal frequency of the control field, $\omega_{\min}$ and $\omega_{\max}$, respectively.

2) Gaussian noise channels: Shannon showed [62], [63], [64] that also in the presence of noise, there exists a non-zero value for the channel capacity $\mathcal{C}$ such that the error in transmitting an infinitely long message can be arbitrarily small. In this case, the limitations to the channel capacity are the bandwidth $\Delta\Omega$ and the power of the noise fields. More formally, the capacity $\mathcal{C}$ of this noisy channel equals to

$$\mathcal{C} = \int_{\omega_{\min}}^{\omega_{\max}} \log_2\left(1+\frac{\phi_f(\omega)}{\varphi_\xi(\omega)}\right)d\omega\,. \tag{24}$$

Thus, for Gaussian white noise Eq. (24) reduces to

$$\mathcal{C} = \Delta\Omega\log_2\left(1+\frac{S}{N}\right), \tag{25}$$

where S/N is given by Eq. (22). The result of Eq. (25) is commonly known as the Shannon-Hartley theorem.

Note that Eq. (24) holds under the assumption that the noise field is a continuous stochastic process sampled from a Gaussian distribution with known variance. However, as also shown in [64], the results for Gaussian noise channels are enough for the general characterization of classical channel capacities, since we can always refer – at least approximately – to the case of arbitrary noise sources by starting from the Gaussian one.

In what follows we present the results of our studies. In particular, we provide tight analytical lower-bounds for the error made in controlling a quantum system subject to arbitrary noise fields. For this purpose, we unify the classical Shannon theory for communication in the presence of noise, the information theoretical analysis of QOC as proposed in [61] (but applied also to colored noise fields) and the Kofman-Kurizki decoherence theory for a quantum system coupled to an environment described by a continuum of levels [19], [20].

VI. Error Limit and Time Bound

In this section we study how the channel capacity of the control problem transforms into a bound for the admissible precision (or error) of the QOC solution as well as a bound on the required time given the control resources. Such a time reflects an information theoretical speed limit that prevents from steering the system faster at given precision.

Following [61], we first introduce $\mathcal{W}$, the set containing all the density operator solutions (i.e. for all admissible control functions $f(t)$) of the SSE describing the dynamics of the system. $\mathcal{W}$ is also denoted as the set of *reachable states* and depends on the initial state ρ_0. $\mathcal{W}$ has dimension $\dim \mathcal{W} \equiv D_{\mathcal{W}}(n)$, which in turn is a function of the dimension n of the system Hilbert space. Next, we introduce a measure for the *complexity* of the optimal control field: D is formally defined as the number of independent degrees of freedom of the control $f(t)$. More practically, D can be equal, for example, to the minimal number of independent bang-bang control pulses [18] or proportional to the bandwidth or sampling points of $f(t)$. In particular, in [61] it has been proven that the information content I_f carried by the control pulse, with I_f proportional to D, cannot be smaller than the product of $D_{\mathcal{W}}$ and $-\log_2(\varepsilon)$, i.e., $I_f \geq -D_{\mathcal{W}} \log_2(\varepsilon)$, where for a control error $\varepsilon \in [0,1]$ (e.g. $\varepsilon = 1 - \mathfrak{F}$), $-\log_2(\varepsilon)$ represents the self-information of ε. Another interpretation is that I_f has to be at least sufficient to specify the $\varepsilon-$ball surrounding the target state. We can rewrite this bound as a lower bound for the control error ε:

$$\varepsilon \geq 2^{-\frac{I_f}{D_{\mathcal{W}}}}. \tag{26}$$

Hence, from $I_f \equiv \mathcal{C}T$, one finds that the minimal time needed to reach a given target state $\hat{\rho}$ in $D_{\mathcal{W}}$ with precision ε is

$$T \geq -\frac{D_{\mathcal{W}}}{\mathcal{C}} \log_2(\varepsilon). \tag{27}$$

Eq. (27) can be interpreted as follows: The amount of information necessary to solve the QOC problem with precision ε under finite channel capacity $\mathcal{C}$ sets a time bound for the system dynamics . As a further step, we derive the formal expression of the control error bound both in the noiseless case and in the presence of white and colored noise.

A. Error bound for a noiseless channel

In the noiseless case, the channel capacity $\mathcal{C}$ is provided by Hartley's law: $\mathcal{C} = \Delta\Omega \log_2(1 + \Delta f/\delta f)$. Thus, $I_f = T\Delta\Omega \log_2(1 + \Delta f/\delta f) = D \log_2(1 + \Delta f/\delta f)$, where we substitute $D = \Delta\Omega\, T$ since the bandwidth $\Delta\Omega$ together with the total time reflects the number of degrees of freedom encoded in the control pulse. Accordingly, by substituting the expression for I_f in Eq. (26), one has

$$\varepsilon \geq \left(1 + \frac{\Delta f}{\delta f}\right)^{-\frac{D}{D_{\mathcal{W}}}}. \tag{28}$$

B. Error bound for Gaussian white noise

Let us now consider a Gaussian white noise source. According to the Shannon-Hartley theorem, in this case the information carried by the control pulse is $I_f = D \log_2(1 + S/N)$, with S/N the signal-to-noise ratio. This entails the following expression for the control error bound:

$$\varepsilon \geq \left(1 + \frac{S}{N}\right)^{-\frac{D}{D_{\mathcal{W}}}}. \tag{29}$$

C. Error bound for Gaussian coloured noise

As explained in Section V-B2, the capacity $\mathcal{C}$ of a channel perturbed by colored Gaussian noise is given by Eq. (24). This means that the information carried by the control pulse is

$$I_f = T \int_{\omega_{\min}}^{\omega_{\max}} \log_2\left(1 + \frac{\phi_f(\omega)}{\varphi_\xi(\omega)}\right) d\omega\,. \tag{30}$$

Hence, this time, we obtain a control error of

$$\varepsilon \geq 2^{-\frac{T}{D_{\mathcal{W}}} \int_{\omega_{\min}}^{\omega_{\max}} \log_2\left(1+\frac{\phi_f(\omega)}{\varphi_\xi(\omega)}\right) d\omega}. \tag{31}$$

VII. Error bounds from perturbation theory

A. The small noise approximation

The Hamiltonian of Eq. (2) can be understood as composed of an (unperturbed) system (described by $H_s(t) = H_d + f(t)H_c(t)$) and a perturbation (described by $H_p(t) = \xi(t)H_n$), that is,

$$H(t) = H_s(t) + H_p(t)\,. \tag{32}$$

If we take only the system Hamiltonian $H_s(t)$ together with the initial state $|\phi_0\rangle$, we obtain a Schrödinger equation with solution $|\phi(t)\rangle$ for the time evolution of the unperturbed system. The time evolution of the perturbed system is described by the state $|\phi_p(t)\rangle$ that is the solution to the Schrödinger equation defined by the perturbed Hamiltonian $H(t)$ and the initial state $|\phi_0\rangle$.

The fidelity of the perturbed dynamics with respect to the unperturbed dynamics is given by $F_p \equiv |\langle\phi(T)|\phi_p(T)\rangle|$. Exploiting Gronwall's lemma [73] we find

$$\||\phi(T)\rangle - |\phi_p(T)\rangle\| \leq \frac{\|H_p\|}{\|H_s\|} \left(\exp\{\|H_s\|T\} - 1\right)\,, \tag{33}$$

where the norms of the Hamiltonians are the time-maximum of the standard operator norm and can be approximated by $\|H_p\|^2 \approx N$ and $\|H_s\|^2 \approx S$. Some algebra yields

$$\||\phi(T)\rangle - |\phi_p(T)\rangle\|^2 = 2 - 2\mathrm{Re}\langle\phi(T)|\phi_p(T)\rangle \tag{34}$$

$$\leq 2 - 2F_p \equiv 2\varepsilon_p\,, \tag{35}$$

where Re stands for the real part. By resolving for the operation error ε_p due to the perturbation (noise) we get the upper bound for the error

$$\varepsilon_p \leq \frac{1}{2}\frac{\|H_p\|^2}{\|H_s\|^2}\left(\exp\left\{\int_0^T \|H_s(t)\|dt\right\} - 1\right)^2 \tag{36}$$

As a first result we can thus state that the operation error ε_p due to a perturbation (i.e. the noise term in Eq. (2)) scales with $\frac{\|H_p\|^2}{\|H_s\|^2} \approx \frac{N}{S}$. If we further assume that without noise we can perfectly control the system, then ε_p is also an upper bound for the control error ε of the noisy system. This is consistent with Eq. (29) for $S/N \gg 1$.

B. Relation with the Kofman-Kurizki decoherence universal formula

The decay of unstable states into a continuum of quantum levels, mimicking a macroscopic reservoir, is well described by the so-called Kofman-Kurizki universal formula [20]. The open dynamics originated by the interaction between a finite-dimensional quantum system and a reservoir leads to decoherence, i.e., the asymptotic loss of the quantum system coherence. We have already seen in Section III and IV that decoherence can be described by modeling the interaction with the reservoir as weak stochastic perturbations. In this regard, the Kofman-Kurizki universal formula, under the hypothesis of weak coupling, predicts how a coherent manipulation of the quantum system modifies its decay rate into the reservoir [21], [25], [74]. This decay rate can also be engineered with optimization techniques to suppress and enhance different coupling modes [25], [27], [28]. Therefore, we phenomenologically expect that the information-time bound of Eq. (27) for the error scaling and the Kofman-Kurizki universal formula for the quantum system decay rate are related. To simplify the derivation, let us consider a two-level system coupled to an arbitrary colored noise field, with Hamiltonian $H(t) = f(t)\sigma_x + \xi(t)\sigma_z$, where $\xi(t)$ denotes the colored noise field with a spectral density $\varphi_\xi(\omega)$. We denote the eigenstates of the Pauli operator σ_x by $|0\rangle$ and $|1\rangle$ and we suppose the system is initially prepared in the state $(|0\rangle + |1\rangle)/\sqrt{2}$. Under the influence of control and noise, the probability to keep the system in its initial state decays as

$$p(t) = \frac{1}{2}(1 + e^{-\chi(t)}) \,, \tag{37}$$

where

$$\chi(t) \equiv \int_0^\infty F(\omega)\varphi_\xi(\omega)d\omega \tag{38}$$

is the so-called decoherence function and $F(\omega)$ is also denoted as filter function and resembles the spectrum of the control pulse. In quantum noise spectroscopy or dynamical decoupling [18], [22], [23], [24], [27], [75], [76], [77], [78], [79], [80], the control pulse is modulated, according to a set of pulse modulation functions, in order to encode information on the noise field in the probability $p(t)$ or to minimize the decoherence function $\chi(t)$, respectively. For a continuous control field $f(t)$ we can introduce the accumulated phase $\theta(t) \equiv \int_0^t f(t')dt'$, and the pulse modulation functions $y(t) = \cos\theta(t)$ and $z(t) = \sin\theta(t)$, so that the filter function is given by $F(\omega) = \frac{4}{\pi}(|Y(\omega)|^2 + |Z(\omega)|^2)$, with $Y(\omega) \equiv \int_0^t y(t')e^{i\omega t'}dt'$ and $Z(\omega) \equiv \int_0^t z(t')e^{i\omega t'}dt'$, where we follow the notation of Ref. [27].

If the control pulse $f(t)$ is designed with the aim to protect the system in its initial state, the control error is given by $\varepsilon = 1 - p$. Thus, after a fixed time T, we can write

$$\varepsilon \approx \frac{1}{2}\chi(T) = \frac{1}{2}\int_0^\infty F(\omega)\varphi_\xi(\omega)d\omega \,, \tag{39}$$

where $e^{-\chi(t)}$ has been approximated as $1 - \chi(t)$ (for a small error). To gain more insight into the scaling of the error with the control resources we make the following approximations: the filter function $F(\omega)$ can be designed to have support only around a central frequency ω_c (e.g. for bang-bang control the filter function has a sinc^2-shape, but also for optimally modulated pulses the bandwidth remains small [25]) and with a small bandwidth if compared to the power spectral density of the stochastic noise field. Thus, we can make the approximation

$$\varepsilon \approx C_0\, \varphi_\xi(\omega_c) \,, \tag{40}$$

with C_0 a constant term depending on the specific choice of the filter function.

Let us now compare this result with the information theoretical limit as given by Eq. (31). Since in practical applications the control pulse is chosen such that the signal-to-noise ratio (evaluated in dB) exceeds a minimum threshold (at least 10-20 dB) that ensures a satisfactory value of the control fidelity $\mathfrak{F}$ (e.g. more than 90%), we can make the approximation $\log_2(1 + \phi_f(\omega)/\varphi_\xi(\omega)) \approx \log_2(\phi_f(\omega)/\varphi_\xi(\omega))$, such that

$$\varepsilon \gtrsim 2^{-\frac{T}{D_\mathcal{W}}\int_{\omega_{\min}}^{\omega_{\max}} \log_2\left(\frac{\phi_f(\omega)}{\varphi_\xi(\omega)}\right)d\omega} .$$

At this point, we also assume that the bandwidth of the control field is smaller than the frequency variation of the power spectral density $\varphi_\xi(\omega)$ of the noise field [1]. As a consequence, the integral $\int_\omega \log_2(\phi_f(\omega)/\varphi_\xi(\omega))\,d\omega$ can be approximated by its integrand $\Delta\Omega\log_2(C_1/\varphi_\xi(\omega_c))$, evaluated at the central frequency ω_c of the effective pulse modulation, together with the characteristic spectral width $\Delta\Omega$. The constant C_1 depends on the precise value and shape of $\phi_f(\omega)$. As a consequence,

$$\varepsilon \gtrsim \left(\frac{\varphi_\xi(\omega_c)}{C_1}\right)^{\frac{\Delta\Omega T}{D_\mathcal{W}}} \approx C_2\,\varphi_\xi(\omega_c) \,, \tag{41}$$

with $D = \Delta\Omega T$ chosen to be of the same order of magnitude than $D_\mathcal{W}$ and $C_2 = 1/C_1$ is a constant [2].

While the above considerations assume that the system should be protected in its initial state, a similar analysis could be made for a state transformation. Indeed, also in this more general case, the filter function $F(\omega)$ has to be chosen in such a way that the decoherence function $\chi(t)$ is minimized. However, this time the constraint of this minimization is not only given by the available resources but also by the requirement that the coherent part of the dynamics leads to the desired state transformation [26]. As a consequence, Eq. (40) will no longer be a small noise approximation, but a lower bound on the control error. We have thus proven that the information-theoretical bound of Eq. (31) leads to the same scaling of the error with the noise as the one obtained in Eq. (40) starting from the Kofman-Kurizki universal decoherence formula.

Example: 1/f-noise: As an example, we consider that the noise field is sampled by a $1/f$ distribution, commonly used to model statistical fluctuations of a wide number of physical and biological systems [9], [10], [11]. As explained in these references, the power spectral density of the $1/f$-noise decays

[1] This assumption is the same that we have made for the filter function $F(\omega)$ to derive the bound in Eq. (40). In this case, $f(t)$ enters the dynamics only through the pulse modulation functions $y(t)$ and $z(t)$ that contain the effective degrees of freedom (see also the arguments in section V-B).

[2] Given a fixed value of the bandwidth $\Delta\Omega$ of the control pulse, $\Delta\Omega T$ is of the same order of magnitude of $D_\mathcal{W}$ if the dimension of the QOC problem saturates the dimension of the set of reachable states.

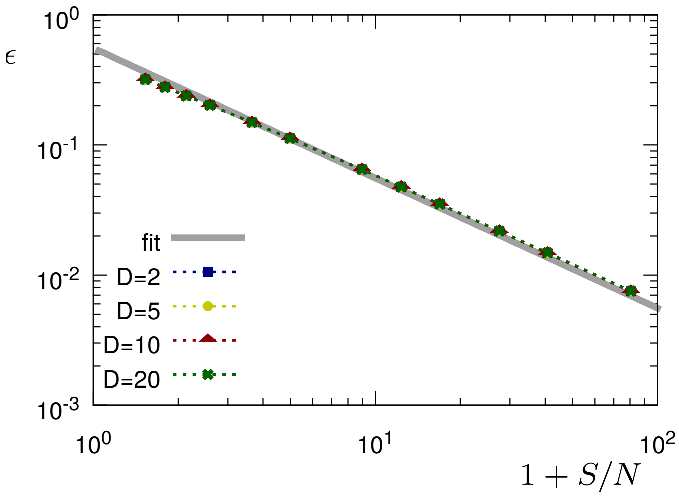

Fig. 1. Dephasing channel (Sec. VIII-A): Control error scaling with respect to signal to noise ratio S/N for different values of D. We choose the parameters $T = 1$, $\omega_y = 2\pi \times 1$, $\omega_z = 2\pi \times 1$. In each optimization, the noise strength γ is chosen as a function of the control pulse power P_f to set the value of S/N. The data points are the minimum error from 10 optimization runs for each value of D, namely ($D = 2$, blue squares), ($D = 5$, yellow circles), ($D = 10$, red triangles), and ($D = 20$, green crosses). The theory curve (grey line, 'bound') shows the result of the fit of the model Eq. (44) as described in the text ($a_1 = 0.53$, $b_1 = 0.001$).

as a power law with the frequency, i.e., $\phi_f(\omega) \propto 1/\omega^\alpha$ where the exponent α is typically in the range $0 < \alpha < 2$ [4]. The case of $\alpha = 1$ is also called pink noise ($1/f$-noise). Thus, the natural choice in this case is to operate the system at high frequency. According to the Kofman-Kurizki universal decoherence formula, when moving to higher frequencies, the error ε decays as $\varepsilon \approx C_0/\omega_c^\alpha$. Likewise, if we consider the error-bound arising from the Shannon-Hartley theorem, we find that $\varepsilon \gtrsim C_2/\omega_c^\alpha$, i.e. confirming the result.

VIII. Examples with Gaussian White Noise

A. Dephasing channel

We consider a two-level system with one control field and the following coherent Hamiltonian:

$$H_1(t) = f(t)\sigma_x + \omega_y\sigma_y + \omega_z\sigma_z, \tag{42}$$

where $f(t)$ is the control field and, as usual, $\{\sigma_x, \sigma_y, \sigma_z\}$ is the set of the Pauli matrices. We add (Gaussian white) noise on the σ_z operator and thus obtain the master equation

$$\dot{\rho} = -i[H_1(t), \rho] + \gamma \begin{pmatrix} 0 & \rho_{12} \\ \rho_{21} & 0 \end{pmatrix}. \tag{43}$$

Our aim is to control at fixed bandwidth $\Delta\Omega$ of the control field $f(t)$ the transfer from the state $\rho_0 = |0\rangle\langle 0|$ to the state $\hat{\rho} = |1\rangle\langle 1|$. We show in Fig. 1 the scaling for the control error ε with respect to the signal-to-noise ratio, where we have optimized the state transfer with dCRAB. In the simulation, we have $D_{\mathcal{W}} = 3$, the dimension of the space of mixed qubit states, $D = \frac{\Delta\Omega}{2\pi}T$ and T the final time of the control operation. We choose the parameters $T = 1$, $\omega_y = \omega_z = 2\pi \times 1$. and the control bandwidth $\Delta\Omega \in 2\pi \times \{2, 5, 10, 20\}$. To fix the signal-to-noise-ratio to the desired value, at each optimization iteration we calculate the signal power $S = P_f$ and set $\gamma = 1/(2T\frac{S}{N})$. This corresponds to a physical model where the noise is induced by a frequency instability of the control pulse proportional to the pulse strength. We can see that the optimization error in this example does not depend on the control bandwidth (except for high signal-to-noise ratios) and that instead the error is dominated by the signal-to-noise ratio. From Eq. (29) we expect

$$\log \varepsilon_1 \gtrsim \log\left(\frac{a_1}{1+\frac{S}{N}} + b_1\right) \tag{44}$$

up to some constants a_1 and b_1. To verify the model from the numerical data we take the data for $D = 20$ and fit the function $\log(\varepsilon_1)$ to the logarithm of the numeric errors. We do the same fit also for alternative model $\log \varepsilon_2 = \log(a_2 \exp(-b_2\frac{S}{N}) + c_2)$. If the fit for the first model produces a lower root-mean-square of the residuals (RMS), this effectively proves our prediction for the scaling of the error. In Fig. 1 we show the fit of ε_1 for which we obtain a RMS of 0.062. If we additionally fit the exponent $-D/D_{\mathcal{W}}$, we obtain $-D/D_{\mathcal{W}} \approx -1.05$ and reduce the RMS to 0.031, while for ε_2 we obtain a RMS of 0.27, confirming our model as well as $-D/D_{\mathcal{W}} \approx -1$. This finding is consistent with the perturbative treatment of the time evolution in Sec. VII-A. Thus, increasing D above the value of $D_{\mathcal{W}}$ saturates the information that can be transferred onto the system and the original exponent can be approximated by $-D/D_{\mathcal{W}} \approx -1$.

B. Decay channel

As a second example, we consider a two-level system with the coherent Hamiltonian $H_2(t) = f(t)\sigma_x + \omega_z\sigma_z$ and a decay term given by the Lindblad superoperator $\mathcal{L}(\rho)$ as follows:

$$\mathcal{L}(\rho) = \gamma\left(a\rho a^\dagger - \frac{1}{2}a^\dagger a\rho - \frac{1}{2}\rho a^\dagger a\right) = \gamma\begin{pmatrix} \rho_{22} & -\frac{1}{2}\rho_{12} \\ -\frac{1}{2}\rho_{21} & -\rho_{22}\end{pmatrix},$$

where $a^\dagger$ and a are the creation and annihilation operators of the qubit excitation and γ is the inverse lifetime of the excited level. We set $T = 1$, $\omega_z = 2\pi \times 2$, $\gamma = 2\pi \times 0.4$ and we then fix the signal power to $\int_0^T f^2(t)dt = (2\pi \times 4)^2$, and thus the signal-to-noise ratio as $S/N = \int_0^T f^2(t)dt/\gamma = 2\pi \times 100$.

We try to optimize the state transfer between a random initial state and a random target state and investigate 100 instances of such random pairs of (pure) states. We optimize each random instance for different values of the bandwidth $\Delta\Omega$. Fig. 2 shows the scaling of the maximum control error (maximized over the random instances of initial and target states) with the bandwidth. Again, we consider two models for the error scaling and fit the parameters. From Eq. (29) we obtain

$$\varepsilon_1 \gtrsim a_1 \exp(-b_1\Delta\Omega) + c_1 \tag{45}$$

up to some constants a_1, b_1 and c_1. To verify the model from the numerical data we fit this model to the data where we exclude the data point for the smallest value of $\Delta\Omega$ as outlier, since for a small bandwidth (virtually constant pulse) the error is influenced by the maximal value of 1. We do the same for an alternative model $\varepsilon_2 = a_2(\Delta\Omega)^{-b_2} + c_2$. In Fig. 2 we show

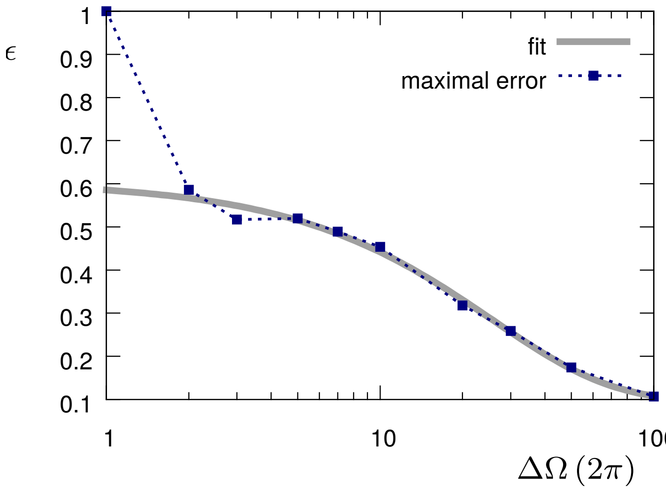

Fig. 2. Decay channel (Sec. VIII-B): Control error scaling with respect to the maximum bandwidth $\Delta\Omega$. The system offers both a decaying and a stable state. The control error is reduced when a higher bandwidth allows faster transitions between the two states. The figure shows the maximal control error over 100 random instances of input and target states (blue squares). If the bandwidth is too low we do not have any control over the system and the maximal error is given by the form of the fidelity function. We fit the error model Eq. (45) to the remaining data points as described in the text (grey solid line, $a_1 = 0.51$, $b_1 = 0.039$, $c_1 = 0.098$).

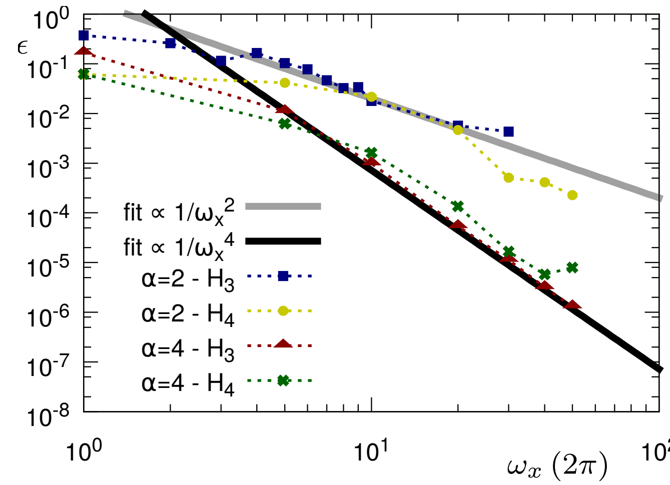

Fig. 3. State protection (Sec. IX-A): Control error scaling with respect to the Rabi frequency ω_x of the driving for $1/f^2$-noise and $1/f^4$ noise and state preservation in $\frac{|0\rangle+|1\rangle}{\sqrt{2}}$. For each of the two types of noise we investigated separately the evolution of the system according to the Hamiltonians H_3 and H_4. The Hamiltonian H_3 includes just the noise and the control and in this case a constant pulse already encodes all possible information. The control error scales with the expected $1/\omega_x^\alpha$ law corresponding to both the information theoretical bound and the analytic decoherence formula. In the second scenario the dynamics is governed by H_4 which includes also static terms in the Hamiltonian and thus a time-modulated control pulse is needed. Yet, the scaling with ω_x^α is still roughly maintained.

the fit of ε_1 for which we obtain a RMS of 0.017, while for ε_2 we obtain a RMS of 0.063.

Note that the bandwidth plays a crucial role here. Indeed, the optimal control strategy in this case is to move the system as fast as possible into the decoherence free subspace (or more precisely in the non-decaying state $|0\rangle\langle 0|$) and to give the system another fast kick right before the end of the time dynamics to steer it into the target state. The higher the admissible bandwidth is, the faster these kicks can be and so the smaller the time the system is exposed to decay and the smaller the control error.

IX. Examples with Gaussian Coloured Noise

To test the analytical results in section VII-B we simulate the time dynamics of one qubit following the Hamiltonian

$$H_3(t) = f(t)\sigma_x + \xi(t)\sigma_z, \quad (46)$$

where $\xi(t)$ is the coloured noise field with spectrum $\varphi_\xi(\omega)$, as well as

$$H_4(t) = f(t)\sigma_x + \omega_y\sigma_y + (\omega_z + \xi(t))\sigma_z. \quad (47)$$

In all cases we set $T = 1$, $\int_0^T f^2(t)dt = \omega_x^2$, $\int_0^T \xi^2(t)dt = 4\pi^2$ and $\omega_y = \omega_z = 2\pi$. We consider two different kinds of noise, i.e. $1/f^\alpha$-noise with $\alpha \in \{2, 4\}$. To simulate the dynamics we generate 20 realizations of each type of noise and solve the SSE for each realization separately. The control objectives are then calculated as the average state overlap from all the 20 realizations.

A. State Protection

First, we consider the case treated analytically in the previous subsections, i.e. we consider an initial state $\frac{|0\rangle+|1\rangle}{\sqrt{2}}$ and try to preserve the system in this state. For the scenario H_3 (i.e. the dynamics is described by the Hamiltonian $H_3(t)$) we keep the pulse $f(t) = \omega_x = \text{const}$. Instead, for the scenario H_4 (i.e. the dynamics is described by the Hamiltonian $H_4(t)$) we try to find an optimal solution $f(t)$ respecting the power constraint and with a pulse modulation corresponding to $D = 10$. Fig. 3 shows the results confirming the expected scaling of the control error with ω_x, i.e. $\varepsilon \gtrsim 1/\omega_x^\alpha$. The numerical data obtained with H_3 is much better described by theory (that was developed for H_3), but also the results from H_4 confirm overall the scaling. To quantify the correspondence between numerical data and simulation we employ the model $\log(\varepsilon) = a + b\log(\omega_x)$ and fit it to the logarithm of the error, where we treat again the smallest value of ω_x as outlier since the error is influenced by the maximal admissible value of 1. From this fit we obtain for the curves the parameter b as an estimate for α. We find $b = 1.7 \pm 0.1$ for ($\alpha = 2$ and H_3), $b = 2.4 \pm 0.3$ for ($\alpha = 2$ and H_4), $b = 4.0 \pm 0.1$ for ($\alpha = 4$ and H_3), $b = 3.3 \pm 0.3$ for ($\alpha = 4$ and H_4). Summarizing, we can clearly distinguish $1/f^2$-noise from $1/f^4$-noise, where the precision is about $0.1 - 0.3$ for H_3 and slightly smaller for H_4.

B. State Transfer

Then, we consider a more general case, where the initial state and the target state are chosen randomly. We examine 50 different random pairs of initial and target states for each set of investigated parameters. We choose the scenario H_4 and fix the pulse energy by setting $\omega_x = 2\pi \times 5$. Then we try to find an optimal choice of the control pulse that minimizes the error of the control problem for different values of the control

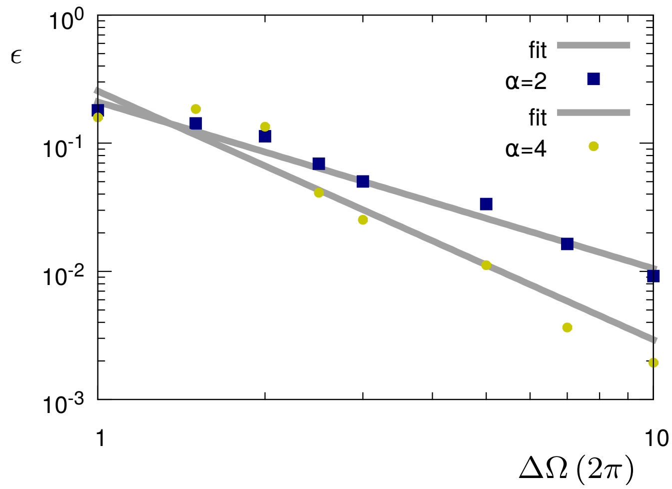

Fig. 4. State transfer (Sec. IX-B): Control error scaling with respect to the bandwidth of the control pulse $\Delta\Omega$ for $1/f^2$-noise and $1/f^4$ noise and state transfer between two random states. The time evolution is given by the Hamiltonian H_4. For each pair of α and $\Delta\Omega$, the figure shows the maximum control error over all pairs of random initial and target states. For both values of α we fit the scaling of the error $\epsilon \propto 1/(\Delta\Omega)^a$ and obtain $a = 1.3$ and $a = 1.9$ for $\alpha = 2$ and $\alpha = 4$, respectively.

bandwidth and for both $1/f^2$- and $1/f^4$-noise. In Fig. 4 we show the numerical results for the maximum error over all instances of random initial and target states for both types of noise and each value of the bandwidth. We expect the error to scale as $\varepsilon \propto 1/(\Delta\Omega)^a$. Numerically we find $a = 1.3$ and $a = 1.9$ for $\alpha = 2$ and $\alpha = 4$, respectively. Due to the more complex dynamics we do not recover exactly the scaling from Fig. 3 or a similar analytic prediction. However, we still find a clear difference in the error scaling for the two types of noise since the fast system modulations can suppress the low frequency noise more efficiently than the high frequency noise. As a consequence, we can conclude that the control resources can be used to operate the system in a regime where it is less affected by the noise. In particular, if the noise power spectral density is decreasing with increasing frequency, increasing the bandwidth of the control (and thus its information content) allows to transform this decreasing noise into a decreasing control error. If the noise decreases faster, also the error scaling is more advantageous and less resources are required to obtain the same control error, compared to a slowly decreasing noise power spectral density.

X. Conclusions

We have studied the error scaling of a quantum control problem as a function of the noise level and control resources from an information theoretical perspective as well as from a dynamic perspective both analytically and numerically. We have shown that the two approaches lead to the same scaling and thus are consistent. To achieve the results we have extended the information theoretical model of Ref. [61] to colored noise and we have investigated numerical examples for both white noise and colored noise to study the relationship between the information theoretical error bounds with the results of optimal control solutions. We have also analytically investigated the dynamics of a quantum system coupled to a temporally correlated environment, with the help of the Kofman-Kurizki universal formula and recovered the same scaling of the control error with the control modulation as predicted by the information theoretical bounds. We expect that our results can pave the way towards an improved design of optimized control pulses for open quantum systems, whereby the optimization is performed also with respect to some environmental features. High fidelity control of open quantum systems is an extremely important ingredient in the emerging field of quantum technologies where one needs to perform precise operations under realistic (noisy) settings.

Acknowledgments

M.M.M and T.C. acknowledge funding from the European Union's Horizon 2020 research and innovation programme under Grant Agreement No. 817482 (PASQuanS), as well as from the Deutsche Forschungsgemeinschaft (DFG, German Research Foundation) under Germany's Excellence Strategy – Cluster of Excellence Matter and Light for Quantum Computing (ML4Q) EXC 2004/1 – 390534769.

M.M.M, S.G. and F.C. acknowledge funding from the Fondazione CR Firenze through the project Q-BIOSCAN.

S.G. and F.C. acknowledge funding from the Fondazione CR Firenze through the project QUANTUM-AI, from the European Union's Horizon 2020 research and innovation programme under Grant Agreement No. 828946 (PATHOS), and from University of Florence through the project Q-CODYCES.

S.M. acknowledges support from the European Union's Horizon 2020 research and innovation programme under the Marie Skłodowska-Curie grant agreement No. 765267 (QuSCo), and No. 817482 (PASQuanS), by the Italian PRIN 2017 and the CARIPARO project QUASAR.

References

[1] H. Breuer, and F. Petruccione, *The Theory of Open Quantum Systems* (Oxford University Press, 2003).

[2] F. Caruso, V. Giovannetti, C. Lupo, and S. Mancini, Quantum channels and memory effects. Rev. Mod. Phys. **86**, 1203 (2014).

[3] E.B. Davies, and J.T. Lewis. An operational approach to quantum probability, Commun. Math. Phys. **17**, 239 (1970).

[4] H.M. Wiseman, Quantum Trajectories and Quantum Measurement Theory. Quantum Semiclass. Opt. **8**, 205-222 (1996).

[5] A. Rivas, and S. Huelga. *Open Quantum Systems: An Introduction* (Spriger Verlag, 2012).

[6] S. Gherardini, S. Gupta, F.S. Cataliotti, A. Smerzi, F. Caruso, and S. Ruffo, Stochastic quantum Zeno by large deviation theory. New J. Phys. **18**, 013048 (2016).

[7] M.M. Müller, S. Gherardini, and F. Caruso, Quantum Zeno Dynamics Through Stochastic Protocols. Annalen der Physik **529** **(9)**, 1600206 (2017).

[8] M.A.C. Rossi, C. Foti, A. Cuccoli, J. Trapani, P. Verrucchi, and M.G.A. Paris. Effective description of the short-time dynamics in open quantum systems. Phys. Rev. A **96**, 032116 (2017).

[9] M.B. Weissman, $1/f$ noise and other slow, nonexponential kinetics in condensed matter. Rev. Mod. Phys. **60**, 537 (1988).

[10] G. Bosman ed., *Noise in Physical Systems and 1/f Fluctuations* (Proceedings of the 16th International Conference, Gainesville, Florida, USA, 2001).

[11] E. Paladino, Y. M. Galperin, G. Falci, and B.L. Altshuler, 1/f noise: Implications for solid-state quantum information. Rev. Mod. Phys. **86**, 361 (2004).

[12] M.M. Müller, S. Gherardini, A. Smerzi, and F. Caruso, Fisher information from stochastic quantum measurements. Phys. Rev. A **94**, 042322 (2016).

[13] M.M. Müller, S. Gherardini, and F. Caruso, Stochastic quantum Zeno-based detection of noise correlations. Sci. Rep. **6**, 38650 (2016).
[14] C.L. Degen, F. Reinhard, and P. Cappellaro, Quantum sensing. Rev. Mod. Phys. **89**, 035002 (2017).
[15] P. Szankowski, G. Ramon, J. Krzywda, D. Kwiatkowski, and L. Cywinski, Environmental noise spectroscopy with qubits subjected to dynamical decoupling. J. Phys.: Condens. Matter **29**, 333001 (2017).
[16] M. Paris, and J. Rehaćek, *Quantum State Estimation* (Springer, Berlin, Heidelberg, Berlin, Germany, 2004).
[17] T.F. Ronnow, Z. Wang, J. Job, S. Boixo, S.V. Isakov, D. Wecker, J.M. Martinis, D.A. Lidar and M. Troyer, Defining and detecting quantum speedup. Science **345** (6195), 420-424 (2014).
[18] L. Viola, E. Knill, and S. Lloyd, Dynamical Decoupling of Open Quantum Systems. Phys. Rev. Lett. **82**, 2417 (1999).
[19] A.G. Kofman, and G. Kurizki, Acceleration of quantum decay processes by frequent observations. Nature **405**, 546–550 (2000).
[20] A.G. Kofman, and G. Kurizki, Universal dynamical control of quantum mechanical decay: modulation of the coupling to the continuum. Phys. Rev. Lett. **87**, 270405 (2001).
[21] G. Gordon, N. Erez, and G. Kurizki, Universal dynamical decoherence control of noisy single- and multi-qubit systems. J. Phys. B **40**, 75 (2007).
[22] M.J. Biercuk, A.C. Doherty, and H. Uys, Dynamical decoupling contruction as a filter-design problem. J. Phys. B: At. Mol. Opt. Phys. **44**, 154002 (2011).
[23] T.J. Green, J. Sastrawan, H. Uys, and M.J. Biercuk, Arbitrary quantum control of qubits in the presence of universal noise. New J. Phys. **15**, 095004 (2013).
[24] G.A. Paz-Silva, and L. Viola, General transfer-function approach to noise filtering in open-loop quantum control. Phys. Rev. Lett. **113**, 250501 (2014).
[25] G, Gordon, G, Kurizki, and D, A. Lidar, Optimal Dynamical Decoherence Control of a Qubit. Phys. Rev. Lett. **101**, 010403 (2008).
[26] J. Clausen, G. Bensky, and G. Kurizki, Task-optimized control of open quantum systems. Phys. Rev. A **85**, 052105 (2012).
[27] M.M. Müller, S. Gherardini, and F. Caruso, Noise-robust quantum sensing via optimal multi-probe spectroscopy. Sci. Rep. **8**, 14278 (2018).
[28] F. Poggiali, P. Cappellaro and N. Fabbri, Optimal Control for One-Qubit Quantum Sensing. Phys. Rev. X **8**(2), 021059 (2018).
[29] V. Jurdjevic, *Geometric control theory* (Cambridge University Press, 1996)
[30] D. D'Alessandro, *Introduction to Quantum Control and Dynamics* (Chapman and Hall/CRC, 2007).
[31] C. Brif, R. Chakrabarti, and H. Rabitz, Control of quantum phenomena: past, present and future. New J. Phys. **12** 075008 (2010).
[32] S.J. Glaser, U. Boscain, T. Calarco, C.P. Koch, W. Köckenberger, R. Kosloff, I. Kuprov, B. Luy, S. Schirmer, T. Schulte-Herbrüggen, D. Sugny, and F.K. Wilhelm, Training Schrödinger's cat: quantum optimal control. The European Physical Journal D **69**, 279 (2015).
[33] C.P. Koch, Controlling open quantum systems: tools, achievements, and limitations. Journal of Physics: Condensed Matter **28**, 213001 (2016).
[34] R. Schmidt, A. Negretti, J. Ankerhold, T. Calarco, and J. T. Stockburger, Optimal Control of Open Quantum Systems: Cooperative Effects of Driving and Dissipation. Phys. Rev. Lett. **107**, 130404 (2011).
[35] V. Mukherjee, A. Carlini, A. Mari, T. Caneva, S. Montangero, T. Calarco, R. Fazio, and V. Giovannetti, Speeding up and slowing down the relaxation of a qubit by optimal control. Phys. Rev. A **88**(6), 062326 (2013).
[36] S. Hoyer, F. Caruso, S. Montangero, M. Sarovar, T. Calarco, M.B. Plenio, and K.B. Whaley, Realistic and verifiable coherent control of excitonic states in a light-harvesting complex. New J. Phys. **16** 045007 (2014).
[37] S. Kallush, M. Kashin, and R. Kosloff. Quantum control with noisy fields, computational complexity versus sensitivity to noise. New J. Phys. **16**, 015008 (2014).
[38] L. Pawela, and Z. Puchala, Quantum control robust with respect to coupling with an external environment. Quantum Inf. Process. **14**, 437-446 (2015).
[39] D.M. Reich, N. Katz and C.P. Koch, Exploiting Non-Markovianity for Quantum Control. Sci. Rep. **5**, 12430 (2015).
[40] V. Mukherjee, V. Giovannetti, R. Fazio, S.F. Huelga, T. Calarco, and S. Montangero, Efficiency of quantum controlled non-Markovian thermalization. New J. Phys. **17**, 063031 (2015).
[41] C. Lovecchio, F. Schäfer, S. Cherukattil, M. Alì Khan, I. Herrera, F.S. Cataliotti, T. Calarco, S. Montangero, and F. Caruso, Optimal preparation of quantum states on an atom-chip device. Phys. Rev. A **93**(1), 010304 (2016).
[42] A. Konnov, and V.F. Krotov, On global methods for the successive improvement of control processes. Avtomatika i Telemekhanika **10**, 77-88 (1999).
[43] N. Khaneja, T. Reiss, C. Kehlet, T. Schulte-Herbrüggen, and S.J. Glaser, Optimal control of coupled spin dynamics: design of NMR pulse sequences by gradient ascent algorithms. J. Magn. Reson. **172**, 296 (2005).
[44] P. Doria, T. Calarco and S. Montangero, Optimal Control Technique for Many-Body Quantum Dynamics. Phys. Rev. Lett. **106**(19), 190501 (2011).
[45] T. Caneva, T. Calarco and S. Montangero, Chopped random-basis quantum optimization. Phys. Rev. A **84**(2), 022326 (2011).
[46] N. Rach, M. M. Müller, T. Calarco, and S. Montangero, Dressing the chopped-random-basis optimization: A bandwidth-limited access to the trap-free landscape. Phys. Rev. A **92**, 062343 (2015).
[47] D.M. Reich, J.P. Palao, and C.P. Koch, Optimal control under spectral constraints: enforcing multi-photon absorption pathways. Journal of Modern Optics **61**, 822 (2014).
[48] F. Motzoi, J.M. Gambetta, S.T. Merkel and F. K. Wilhelm, Optimal control methods for rapidly time-varying Hamiltonians. Phys. Rev. A **84**, 022307 (2011).
[49] J.J.W.H. Sørensen, M.O. Aranburu, T. Heinzel, and J.F. Sherson, Quantum optimal control in a chopped basis: Applications in control of Bose-Einstein condensates. Phys. Rev. A **98**, 022119 (2018).
[50] S. van Frank, A. Negretti, T. Berrada, R. Bücker, S. Montangero, J.F. Schaff, T. Schumm, T. Calarco, and J. Schmiedmayer, Interferometry with non-classical motional states of a Bose–Einstein condensate. Nature Communication **5**, 4009 (2014).
[51] A. Omran, H. Levine, A. Keesling, G. Semeghini, T.T. Wang, S. Ebadi, H. Bernien, A.S. Zibrov, H. Pichler, S. Choi, J. Cui, M. Rossignolo, P. Rembold, S. Montangero, T. Calarco, M. Endres, M. Greiner, V. Vuletić, and M.D. Lukin, Generation and manipulation of Schrödinger cat states in Rydberg atom arrays. Science **365**, 570-574 (2019).
[52] S. Rosi, A. Bernard, N. Fabbri, L. Fallani, C. Fort, M. Inguscio, T. Calarco, and S. Montangero, Fast closed-loop optimal control of ultracold atoms in an optical lattice. Phys. Rev. A **88**(2), 021601 (2013).
[53] F. Frank, T. Unden, J. Zoller, R.S. Said, T. Calarco, S. Montangero, B. Naydenov and F. Jelezko, Autonomous calibration of single spin qubit operations. npj Quantum Information **3**, 48 (2017).
[54] R. Heck, O. Vuculescu, J.J. Sørensen, J. Zoller, M.G. Andreasen, M.G. Bason, P. Ejlertsen, O. Elíasson, P. Haikka, J.S. Laustsen, L.L. Nielsen, A. Mao, R. Müller, M. Napolitano, M.K. Pedersen, A.R. Thorsen, C. Bergenholtz, T. Calarco, S. Montangero, and J.F. Sherson, Remote optimization of an ultracold atoms experiment by experts and citizen scientists. Proceedings of the National Academy of Sciences **115** (48), E11231-E11237 (2018).
[55] N. Margolus, L.B. Levitin, The maximum speed of dynamical evolution. Physica D **120** (1-2), 188-195 (1998).
[56] S. Deffner and S. Campbell, Quantum speed limits: from Heisenberg's uncertainty principle to optimal quantum control. J. Phys. A: Math. Theor. **50**, 453001 (2017).
[57] S. Deffner and E. Lutz, Quantum speed limit for non-Markovian dynamics. Phys. Rev. Lett. **111**, 010402 (2013).
[58] T. Caneva, M. Murphy, R. Calarco, R. Fazio, S. Montangero, V. Giovannetti and G.E. Santoro, Optimal control at the quantum speed limit. Phys. Rev. Lett. **103**, 240501 (2009).
[59] K.W. Moore and H. Rabitz, Exploring constrained quantum control landscapes. J. Chem. Phys. **137**, 134113 (2012).
[60] T. Caneva, A. Silva, R. Fazio, S. Lloyd, T. Calarco and S. Montangero, Complexity of controlling quantum many-body dynamics. Phys. Rev. A **89**, 04322 (2014).
[61] S. Lloyd, and S. Montangero, Information Theoretical Analysis of Quantum Optimal Control. Phys. Rev. Lett. **113**, 010502 (2014).
[62] T.M. Cover, and J.A. Thomas, *Elements of Information Theory* (Wiley-Interscience New York, NY, USA, 2006).
[63] C.E. Shannon, A Mathematical Theory of Communication. The Bell System Technical Journal **27**, 623-656 (1948).
[64] C.E. Shannon, Communication in the Presence of Noise. Proceedings of the IRE **37** **(1)**, 10-21 (1949).
[65] S. Gherardini, M.M. Müller, S. Montangero, T. Calarco, and F. Caruso, Information flow and error scaling for fully-quantum control. In preparation (2020).
[66] B. Bylicka, D. Chruscinski and S. Maniscalco, Non-Markovianity and reservoir memory of quantum channels: a quantum information theory perspective. Sci. Rep. **4**, 5720 (2014).
[67] A. Uhlmann. The "transition probability" in the state space of a *-algebra. *Reports on Mathematical Physics* **9** (2), 273-279 (1976).

[68] J.A. Nelder and R. Mead, A Simplex Method for Function Minimization. The Computer Journal 7(4), 308-313 (1965)

[69] R. Chakrabarti, and H. Rabitz, Quantum control landscapes. International Reviews in Physical Chemistry **26 (4)**, 671-735 (2007).

[70] R.V.L. Hartley, Transmission of Information1. Bell System Technical Journal, 7: 535-563 (1928).

[71] N.G. Van Kampen, *Stochastic Processes in Physics and Chemistry* 3rd edition (Elsevier, 2007).

[72] S.M. Kay, *Fundamentals of Statistical Signal Processing* (Prentice Hall, 2001).

[73] T.H. Gronwall, Note on the derivatives with respect to a parameter of the solutions of a system of differential equations. Ann. of Math., 20 (2): 292–296 (1919).

[74] A. Zwick, G.A. Alvarez, and G. Kurizki, Maximizing Information on the Environment by Dynamically Controlled Qubit Probes. Phys. Rev. Applied **5**, 014007 (2016).

[75] T. Yuge, S. Sasaki, and Y. Hirayama, Measurement of the noise spectrum using a multiple-pulse sequence. Phys. Rev. Lett. **107**, 170504 (2011).

[76] G.A. Alvarez, and D. Suter, Measuring the Spectrum of Colored Noise by Dynamical Decoupling. Phys. Rev. Lett. **107**, 230501 (2011).

[77] J. Bylander, S. Gustavsson, F. Yan, F. Yoshihara, K. Harrabi, G. Fitch, D.G. Cory, Y. Nakamura, J.-S. Tsai, and W.D. Oliver, Noise spectroscopy through dynamical decoupling with a superconducting flux qubit. Nat. Phys. **7**, 565-570 (2011).

[78] L.M. Norris, G.A. Paz-Silva, and L. Viola, Qubit noise spectroscopy for non-Gaussian dephasing environments. Phys. Rev. Lett. **116**, 150503 (2016).

[79] V.M. Frey, S. Mavadia, L.M. Norris, W. de Ferranti, D. Lucarelli, L. Viola, and M.J. Biercuk, Application of optimal band-limited control protocols to quantum noise sensing. Nat. Comm. **8**, 2189 (2017).

[80] H.-V. Do, C. Lovecchio, I. Mastroserio, N. Fabbri, F.S. Cataliotti, S. Gherardini, M.M. Müller, N. Dalla Pozza, and F. Caruso, Experimental proof of Quantum Zeno-assisted Noise Sensing. New J. Phys. **21**, 113056 (2019).